J Vet Sci. 2019 Nov;20(6):e62
https://doi.org/10.4142/jvs.2019.20.e62
pISSN 1229-845X·eISSN 1976-555X

Journal of Veterinary Science

Original Article
Medical Imaging

Check for updates

Semi-quantitative strain elastography may facilitate pre-surgical prediction of mandibular lymph nodes malignancy in dogs

Mihyun Choi [1,2], **Junghee Yoon**[2], **Mincheol Choi** [2,*]

[1]Haemaru Referral Animal Hospital, Seongnam 13590, Korea
[2]Department of Veterinary Medical Imaging, College of Veterinary Medicine, Seoul National University, Seoul 08826, Korea

OPEN ACCESS

Received: Jul 9, 2019
Revised: Sep 25, 2019
Accepted: Oct 4, 2019

***Corresponding author:**
Mincheol Choi
Department of Veterinary Medical Imaging, College of Veterinary Medicine, Seoul National University, 1 Gwanak-ro, Gwanak-gu, Seoul 08826, Korea.
E-mail: mcchoi@snu.ac.kr

© 2019 The Korean Society of Veterinary Science
This is an Open Access article distributed under the terms of the Creative Commons Attribution Non-Commercial License (https://creativecommons.org/licenses/by-nc/4.0) which permits unrestricted non-commercial use, distribution, and reproduction in any medium, provided the original work is properly cited.

ORCID iDs
Mihyun Choi
https://orcid.org/0000-0001-9066-2574
Mincheol Choi
https://orcid.org/0000-0002-3456-4790

Funding
This study was supported by the Research Institute for Veterinary Science at Seoul National University and the Haemaru Referral Animal Hospital. The authors thank the staff of the Veterinary Medical Imaging Department, Haemaru Referral Animal Hospital for assistance during inter-observer analysis.

Conflict of Interest
The authors declare no conflicts of interest.

ABSTRACT

Evaluation of mandibular lymph nodes in a patient with head and neck cancer is important for stage determination and prognosis development, and, in human medicine, the use of sonoelastography for differentiating between non-metastatic and metastatic lymph nodes has been reported. Our prospective, cross-sectional study aimed to evaluate the diagnostic performance of strain elastography and to determine elastographic cut-off values for predicting malignancy. Sixty-six mandibular lymph nodes were included (clinical healthy, n = 45; non-metastatic, n = 8; and metastatic, n = 13). Elastographic images were evaluated qualitatively (elastographic pattern) and semi-quantitatively (mean hue histogram and stiffness area ratios). Elastographic patterns were classified as grades 1 to 4, according to the percentage of high elasticity determined by visualization. The mean hue histogram was defined based on as the mean pixel color values within the lymph node. Stiffness area ratios were determined by computer program analysis of the stiff area. Among the criteria, receiver operating characteristic curve analyses revealed cut-off values for the prediction of malignancy of 92.26 for mean hue histogram (sensitivity: 100%, specificity: 92%), and 0.17 for stiffness area ratios (sensitivity: 86%, specificity of 100%). Reproducibility and repeatability were excellent. In conclusion, semi-quantitative evaluation via strain elastography holds potential for predicting lymph node malignancy.

Keywords: Lymph node; predicting malignancy; stiffness area ratio; strain histogram; ultrasound elastography

INTRODUCTION

Assessment of regional lymph nodes is important for staging head and neck cancers, as well as for establishing their prognosis [1]. Although the rates of lymph node metastasis vary with tumor type, histologic grade, and location, increased tumor size has been identified as a global negative prognostic factor [2]. Manual palpation of lymph nodes has generally been promoted in veterinary medicine; however, more than 85% of dogs with lymph node metastasis are not diagnosed [3], and cytological or histopathological examination is required for accurate metastasis evaluation [4]. Multiple imaging techniques such as

Generated by xmlinkpress

Author Contributions

Conceptualization: Choi M[1], Yoon J, Choi M[2]; Data curation: Choi M[1], Lee G; Formal analysis: Choi M[1], Lee G; Investigation: Choi M[1], Lee G; Methodology: Choi M[1], Lee G; Supervision: Choi M[2]; Validation: Choi M[2]; Visualization: Choi M[1]; Writing - original draft: Choi M[1]; Writing - review & editing: Choi M[1], Yoon J, Choi M[2].

Choi M[1], Mihyun Choi; Choi M[2], Mincheol Choi.

ultrasonography, computed tomography, and magnetic resonance imaging can also be used to detect abnormal lymph nodes [5-11], however, overlapping results for diagnosing metastasis [5-7], the requirement for general anesthesia [8-11], and the use of ionizing radiation in computed tomography [9,10], are critical limitations. Therefore, non-invasive, simple imaging techniques are required for the pre-surgical assessment of patients with head and neck cancers.

Elastography is an imaging modality used to map the elastic properties of soft tissues [12]. Malignant tissues tend to be stiffer than normal tissues as they contain an increased density of tumor cells and vasculature, as well as fibrotic material [13-16]. Given these properties, elastography has been used to assess various organs for malignancy in human medicine [12-18]. The successful use of strain elastography for qualitative analysis of lymph nodes has also been reported in veterinary medicine [7,19], however, to our knowledge, evaluation of mandibular lymph nodes using semi-quantitative elastography for predicting malignancy has not been reported in veterinary medicine.

The present study aimed to evaluate the diagnostic performance of strain elastography and determine elastographic cut-off values for predicting mandibular lymph node malignancy by using qualitative and semi-quantitative strain elastography. The hypothesis was that strain elastography would differ among clinically healthy, non-metastatic, and metastatic lymph nodes.

MATERIALS AND METHODS

Animals

This study had a prospective, cross-sectional design. Client-owned dogs were included in the September 2017 to December 2018 study. All procedures were performed according to the Ethical Principle in Animal Research adopted by the Seoul National University and were approved by the Seoul National University Institutional Animal Care and Use Committee (SNU-170912-24). Owners signed consent forms before the study. Dogs were classified as clinical healthy based on routine physical examination, complete blood analysis (including complete blood count, biochemical profile and C-reactive protein level), radiologic examination (thoracic radiography and abdominal ultrasonography), and the absence of any known malignancy. The patient group included dogs whose owners agreed to allow cytological or histopathological confirmation of mandibular lymph nodes and primary head and/or neck cancer. Lymph nodes with non-diagnostic cytology results (low cellularity or unclear diagnosis) were excluded.

Ultrasound procedure

Mandibular lymph nodes were examined using grey-scale ultrasound and then by strain elastography. The procedures were performed while the dogs were awake. Examinations were performed by the first author using a 2–12 MHz linear probe (Arietta 60, Hitachi-Aloka, Japan) in lateral recumbency. For mandibular lymph node imaging, B-mode images in the longitudinal plane were obtained first, and thereafter, the imaging mode was changed to the elastography mode. For the clinically healthy group, the left mandibular lymph nodes were imaged, while for the patient group, the mandibular lymph nodes ipsilateral to the mass were imaged. When patients had multiple enlarged lymph nodes, all lymph nodes were examined. Following the elastographic examination, fine needle aspirates (FNAs) were obtained under ultrasound guidance using 24-gauge needles or surgical biopsy of

the mandibular lymph node was performed. The lymph nodes in the patient group were classified as non-metastatic or metastatic.

For strain elastography, compression with light pressure followed by decompression was applied repeatedly until a stable image was obtained. The direction of compression was upwards and then downwards. Real-time elastographic and B-mode images simultaneously appeared side-by-side on the screen. Regions-of-interest (ROIs) included the target lymph nodes, but excluded other tissues (e.g., bone, blood vessels) that may disturb analysis of the relative stiffness of the target lymph nodes. At least three elastographic images were obtained. All ultrasound elastographic images were displayed using 256-color mapping of each pixel according to the degree of strain with the color scale ranging from red (highest strain, softest) to, green (average strain, intermediate), to blue (no strain, hardest). All images were sent to a picture archiving and communication system (PACS; INFINITT, Infinitt Healthcare Co., Ltd., Korea) and were then saved as bit-map files for later analysis.

Image analysis

Ultrasonographic images for each dog were anonymized and randomized; the corresponding cytological or histopathological results were blinded for evaluation. All images were reviewed by two observers. The B-mode images were evaluated on the basis of the size and, shape of the lymph node, presence of the hyperechoic hilum, margin type, and echogenicity. The width (cm) of the lymph node was evaluated to determine size. Width-to-depth ratio was used to determine shape. The lymph node margins were classified as irregular or smooth. Lymph node echogenicity was classified as hypoechoic or isoechoic as compared to that of adjacent fat.

Strain elastographic images were evaluated qualitatively and semi-quantitatively. If an anechoic structure (suspected cystic or necrotic changes) was detected in the parenchyma, it was not included in the analysis because these are not indicative of a solid component. For qualitative analysis, the elastographic patterns were classified based on the distribution and percentage of the lymph node area to the hardness area (blue). Grade 1 indicated absent or very low stiffness (i.e., blue); grade 2 indicated a stiff area comprising < 50% of the lymph node; grade 3 indicated a stiff area comprising > 50% of the lymph node; and grade 4 indicated a lymph node with predominant stiffness that occupied the entire lymph node space (**Fig. 1**) [18].

For semi-quantitative analyses, computer-aided analyses of the mean hue histogram values and stiffness area ratios in the acquired images were performed. The mean hue histogram [20] and stiffness area ratios [21] were assessed off-line using Image J software (National Institutes of Health, USA). The mean hue histogram (**Fig. 2**) was constructed using the mean pixel color values within the lymph node via the software plug-in for hue histogram analysis. First, color-coded images were obtained by subtracting grey-scale images from the original elastographic images to eliminate B-mode information. Second, ROIs were drawn manually around the entire lymph node in the B-mode images. These ROIs were superimposed onto the color-coded images and mean hue histograms were constructed.Values range from 0 to 255 (from red to green to blue), and the increasing stiffness resulted in an increased mean hue histogram value. Stiffness area ratios (**Fig. 3**) were determined using the following image processing steps. First, ROIs were manually selected to include the lymph node. Second, the stiffer tissue was visualized as a colored pixel determined to be within a certain threshold level (hue: 145–180, brightness: 0–255). The stiff tissue areas were indicated with red pixels, and the percentage of the stiff tissue area within the ROI was calculated.

https://doi.org/10.4142/jvs.2019.20.e62

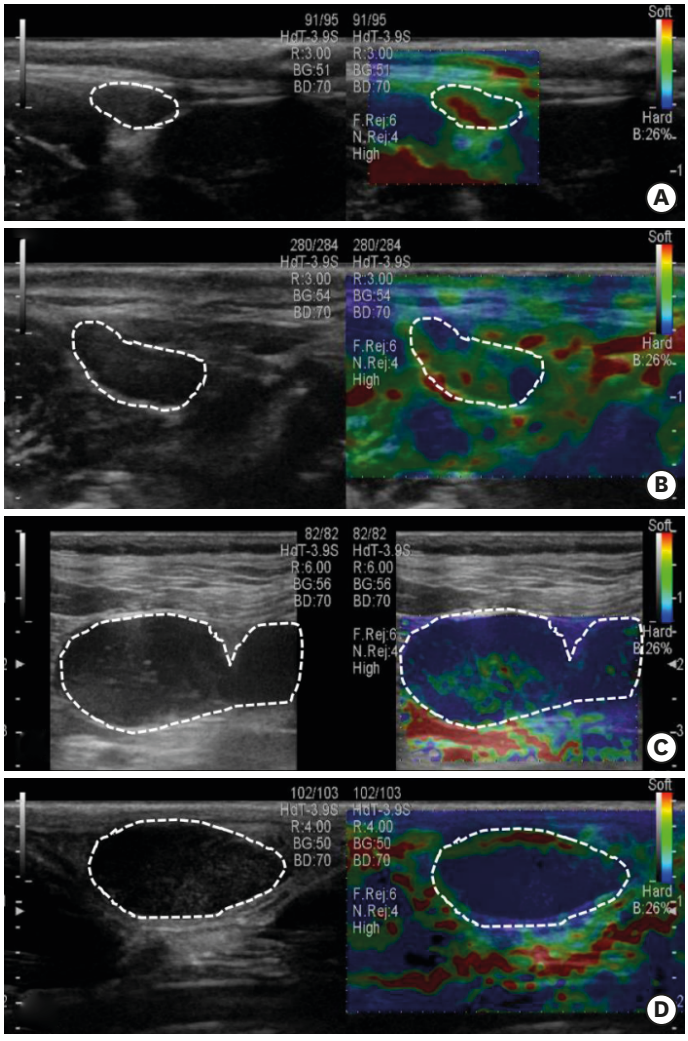

Fig. 1. Elastographic pattern used to assess lymph nodes. (A) Grade 1, predominantly red and green areas and, rarely, blue areas; (B) grade 2, predominantly red and green areas with blue area comprising < 50%; (C) grade 3, predominantly green and blue areas with blue areas comprising > 50%; (D) grade 4, predominantly blue area comprising nearly 100% (lymph node outlined with a dotted line).

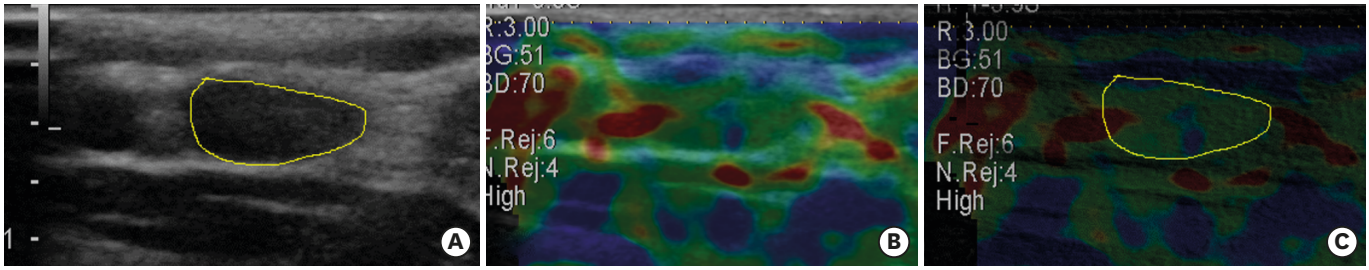

Fig. 2. Evaluated mean hue histogram. From original images (A and B), a subtracted (B – A) color-code image (C) with a region of interest around the lymph node was obtained and the mean hue histogram analyzed.

After B-mode and strain elastography image analysis, the results were classified into three groups (clinically healthy, non-metastatic, or metastatic lymph node) based on cytological or histopathological examinations, and statistical analyses were performed. Strain elastography was performed three times for each lymph node and the values were averaged for analysis. If

https://doi.org/10.4142/jvs.2019.20.e62

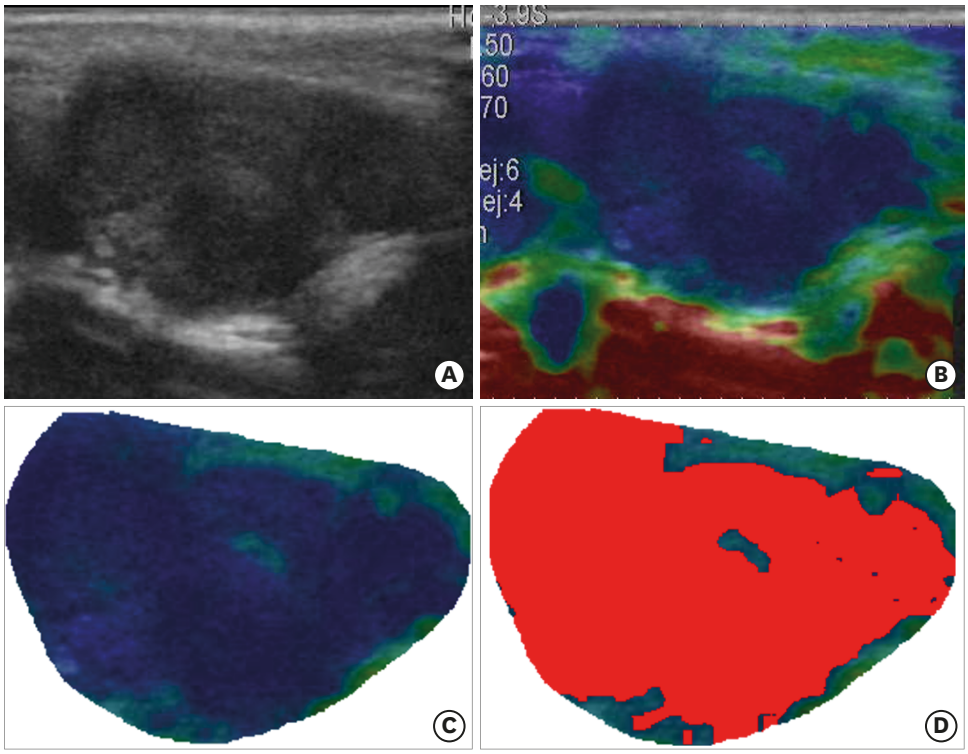

Fig. 3. Calculated stiffness area ratios. From a binary image (A and B), the lymph node area was manually selected as the region of interest (C), and the stiffer tissue visualized as a red pixel (D) was determined within specific threshold levels (hue: 145–180, brightness: 0–255).

the patient had enlargement of multiple lymph nodes, all lymph nodes were analyzed and the average calculated.

Statistical analysis

Statistical analysis using SPSS software (IBM SPSS Statistics 22, IBM Corporation, USA). Normal distribution of quantitative variables was determined by the Kolmogorov-Smirnov test. Normally distributed data were presented as a mean ± standard deviation (SD). Quantitative variables including size, width-to-depth ratio, mean hue histogram and stiffness area ratios were compared across groups using one-way analysis of variance (ANOVA). Qualitative variables including presence of hyperechoic hilum, margin, parenchymal echogenicity, and elastographic pattern, were compared using a Kruskal-Wallis test. Bonferroni corrected Mann-Whitney tests were performed for post hoc multiple comparisons when significant differences were identified by ANOVA or Kruskal-Wallis test.

To evaluate the diagnostic performance of the variables that were significantly different between non-metastatic and metastatic lymph nodes, optimal cut-off values were determined using receiver operating characteristic (ROC) curves. All values were determined using the Youden index. Areas under the curve (AUCs) were calculated with 95% confidence intervals (CIs) to quantify the ability of each variable to detect malignancy. Assessments of inter- and intra-observer agreement in the qualitative data analyses were performed using Kappa statistics and quantitative data were analyzed using intra-class correlations (ICC). The strength of an agreement was classified based on k values: poor (k: < 0.04), moderate (0.41–0.6), good (0.61–0.79), and excellent (> 0.8) [22]. A p value of < 0.05 was considered statistically significant.

https://doi.org/10.4142/jvs.2019.20.e62

RESULTS

The clinically healthy group included 45 dogs and the patient group included 12 dogs. One patient was excluded because of the presence of non-diagnostic cytology results. The details of the clinically healthy group are as follows: median age of 3 years (range: 1–12 years); eight females, 11 spayed females, three males and 23 castrated males; and the included breeds were Beagle (n = 10), Maltese (n = 9), toy Poodle (n = 6), mixed (n = 5), Chihuahua (n = 3), Dachshund (n = 3), Shih-Tzu (n = 3), Pomeranian (n = 2), Cavalier King Charles spaniel (n = 1), Coton de Tulear (n = 1), miniature Schnauzer (n = 1) and Spitz (n = 1). The details of the patient group is as follows: median age of 13 years (range: 2–15 years); three females, five spayed females, one male, and two castrated males; and the included breeds were Maltese (n = 5), English Cocker spaniel (n = 2), Borzoi (n = 1), miniature Schnauzer (n = 1), Scottish terrier (n = 1), and Pomeranian (n = 1). Among the patients, 21 ipsilateral mandibular lymph nodes were evaluated. According to cytology (n = 19) or histopathology (n = 2) results, examined lymph nodes were categorized as metastatic (n = 13) or non-metastatic (n = 8).

Sonographic lymph node results are summarized in **Table 1** and elastographic lymph node findings are summarized in **Table 2**. On grey-scale ultrasonography, there were significant differences ($p < 0.05$) in width-to-depth ratio > 0.5 for metastatic lymph nodes compared to clinically healthy and non-metastatic nodes. Otherwise, no statistically significant difference was detected for depth, parenchymal echogenicity, irregular margin type, and hyperechoic hilum definition. However, increased lymph node depth and absence of hyperechoic hilum were more frequent in metastatic nodes. Elastographic patterns, mean hue histogram values and stiffness area ratios were significantly different between metastatic lymph nodes and non-metastatic and clinically healthy lymph nodes ($p < 0.01$). Clinically healthy and non-metastatic lymph nodes were either elastographic pattern grade 1 or 2, reflecting relatively

Table 1. The B-mode characteristics of the conventional ultrasonography-evaluated criteria for the different lymph nodes study groups

Characteristics	Clinically healthy (n = 45)	Non-metastatic (n = 8)	Metastatic (n = 13)
Depth (cm)	0.37 ± 0.11	0.85 ± 0.65	0.95 ± 0.51
Width-to-depth ratio			
< 0.5	39 (85)	5 (100)	4 (57)
> 0.5	6 (15)	0 (0)	3 (43)
Hyperechoic hilum			
Present	27 (60)	2 (40)	1 (14)
Absent	18 (40)	3 (60)	6 (86)
Echogenicity			
Normal	45 (100)	4 (80)	1 (14)
Abnormal	0 (0)	1 (20)	6 (86)
Margin			
Smooth	45 (100)	5 (100)	5 (71)
Irregular	0 (0)	0 (0)	2 (29)

Values are presented as mean ± standard deviation or number (percent).

Table 2. Qualitative analysis of strain elastographic characteristics of clinically healthy, non-metastatic, and metastatic lymph nodes

Criteria	Clinically healthy (n = 45)	Non-metastatic (n = 8)	Metastatic (n = 13)
Elastographic pattern	1.56 ± 0.50	1.50 ± 0.53	3.31 ± 0.85
Mean hue histogram	81.48 ± 7.86	86.99 ± 4.73	101.35 ± 8.80
Stiffness area ratio	0.03 ± 0.02	0.05 ± 0.06	0.41 ± 0.20

Values are presented as mean ± standard deviation.

https://doi.org/10.4142/jvs.2019.20.e62

Table 3. Diagnostic performance of B-mode and strain elastography parameters in predicting malignancy in mandibular lymph nodes

Criteria	AUC	95% CI	*p* value	Cut-off	Sensitivity (%)	Specificity (%)	Youden Index
Mean hue histogram	0.982	0.878–1.000	< 0.01	> 92.26	100	91.89	0.92
Elastographic pattern	0.902	0.763–0.974	< 0.01	> 2	85.71	100	0.86
Stiffness area ratio	0.879	0.735–0.961	< 0.01	> 0.17	85.71	100	0.86
Width-to-depth ratio	0.661	0.492–0.804	0.1591	> 0.48	57.14	77.50	0.35

AUC, area under the curve; CI, confidence interval.

soft elasticity. Metastatic lymph nodes were mostly hardness grade 3 or 4, reflecting relatively stiff elasticity, except for one lymph node.

The diagnostic performance of B-mode and elastography variables are summarized in **Table 3**. The ROC analyses revealed that the best cut-off values for the prediction of metastatic lymph nodes were 92.26 for the mean hue histogram ($p < 0.01$; with a sensitivity of 100% and specificity of 92%), 0.17 for stiffness area ratios ($p < 0.01$; with a sensitivity of 86% and specificity of 100%), and grade 2 for elastographic pattern ($p < 0.01$; with a sensitivity of 86% and specificity of 100%). Among the variables, the mean hue histogram values showed the highest AUC, 0.982 (95% CI, 0.878–1.000) (**Fig. 4**).

Kappa values for elastographic patterns had an inter-observer and intra-observer variability of 0.53, and 0.87, respectively, indicating moderate reproducibility and excellent repeatability. The ICC between observers was 0.882 (0.755–0.943) for the mean hue histogram and 0.868 (0.675–0.946) for stiffness area ratios, indicating excellent inter-observer reproducibility. Furthermore, the ICC for each observer was 0.928 (0.851–0.965) for the mean hue histogram and 0.995 (0.987–0.998) for the stiffness area ratios, indicating excellent intra-observer repeatability.

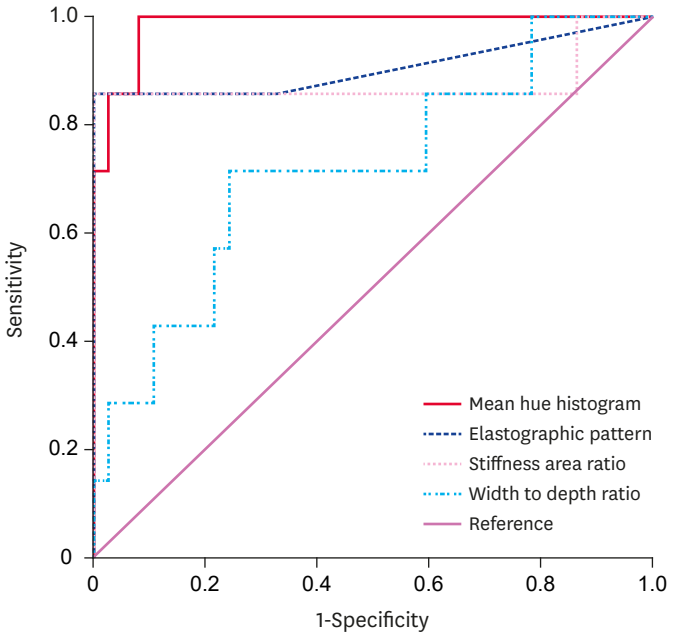

Fig. 4. Receiver operating characteristic curve assessment of the diagnostic efficacy of grey-scale ultrasonography and strain elastography for predicting mandibular lymph node malignancy. Area under the curve for the mean hue histogram (0.982) is higher than those for the elastographic pattern (0.902), the stiffness area ratio (0.879), and the width-to-depth ratio (0.661).

https://doi.org/10.4142/jvs.2019.20.e62

DISCUSSION

Grey-scale ultrasonography is frequently used to assess lymph nodes in cancer patients [6]. Although the use of diagnostic criteria such as lymph node size, shape, parenchymal echogenicity, margination, and vascular pattern have been reported [5,23,24], the utility and specificity of these criteria for identifying metastatic lymph nodes remains unclear.

In the present study, we evaluated the usefulness of various criteria of grey-scale ultrasonography and strain elastography criteria. Although a significant difference was observed for width- to-depth ratio, most grey-scale ultrasonographic features, including width, parenchymal echogenicity, irregular margin, and hyperechoic hilum definition were not significantly different among the study groups. Notably, all strain elastography criteria had higher AUC values than those of grey-scale ultrasonography.

To our knowledge, no previous study has reported the use of the semi-quantitative strain elastography for predicting malignancy of mandibular lymph nodes. Elastographic patterns are often used as superficial lymph node diagnostic criteria in veterinary medicine, offering 80%–100% sensitivity and 75%–96% specificity [19]. We also observed that elastographic patterns had high AUC values; however, this was relatively dependent on the examiner ($k = 0.53$). Our results indicated that semi-quantitative criteria, such as the mean hue histogram and stiffness area ratios, were useful, and providing high repeatability and reproducibility. The cut-off values for predicting malignancy were a mean hue histogram values > 92.26 and a stiffness area ratio > 0.17.

We did not evaluate strain ratios in the present study because only a fixed ROI box could be used in our device. In a human study using ultrasound elastography, a strain ratio > 1.5 was the most useful for metastatic lymph node classification [18]. Our study showed that in clinically healthy dogs and in some patients, the mandibular lymph nodes were often too small, whereas in patients with lymph node enlargement, the nodes often exhibited a heterogeneous pattern, making it difficult to select where to position the ROI. However, by using Image J to determine the mean histogram values it was possible to utilize freely drawn ROIs. As in a previous report, mean hue histogram values were found to be equal to strain ratio for diagnostic performance [25], thus, we evaluated only the mean hue histograms in this study.

Imaging of human cervical lymph nodes using strain elastography has revealed that the cortex of the lymph node is harder than the hilum and medulla [26,27]. Inflammatory lymph nodes have an elastographic appearance similar to that of a normal lymph node, but with a stiffer cortex and a softer hilum [27]. The cortex of malignant lymph nodes is harder than the cortex of normal nodes and typically harder than its medulla [27], because metastatic cancer cells invade the lymph nodes through afferent lymphatic vessels, moreover, the metastatic focus initially forms in the peripheral region, remote from the hilum of the lymph node [4]. In the present study, however, we were unable to differentiate between the cortex and the medulla in all groups. The reason for this inability may be that the nodes were too small to differentiate their anatomic structure, shear-wave elastographic examination may be needed to focus on the cortex and medulla of such lymph nodes.

In this study, strain elastography yielded some false-positive or -negative results. One patient produced a false-negative result, but we did not perform a histopathologic examination as the cause was suspected to be early-stage metastasis. Furthermore, there was a focal anechoic

lesion in the lymph node parenchyma, suggestive of necrosis, a cyst, or a highly vascularized structure that can result in a false-negative result in strain elastography [19]. Strain elastography is operator-dependent; thus, if the ROI does not adequately represent the tissue of interest and its surroundings or if there is a size discrepancy between the lesion and the surrounding tissue, assessments of lymph nodes stiffness may be incorrect or limited [28].

The limitations of the present study include its inclusion of a small number of patients within each cytological diagnosis group. Based on our results, a larger-scale study that incorporates a histologic confirmation approach and included a variety of tumor types is required. Furthermore, our clinically healthy dogs were selected based on clinical examination (physical examination, blood analysis and imaging studies) in order to avoid the use of invasive procedures, such as FNA or biopsy, thus, we could not elucidate the homogeneity of the clinically healthy group.

In conclusion, our results suggest that semi-quantitative strain elastography with its high sensitivity and specificity, may be helpful for pre-surgical prediction of mandibular lymph nodes malignancy in patients with head and neck cancer. Variables, such as the mean hue histogram value and a stiffness area ratio, which offered the highest diagnostic accuracy in our study, can be used as an aid when determining the need for further examination such as that incorporating FNA or biopsy. Further larger prospective studies utilizing histopathological confirmation of elastographic observations are necessary to improve the accuracy of this approach.

REFERENCES

1. Herring ES, Smith MM, Robertson JL. Lymph node staging of oral and maxillofacial neoplasms in 31 dogs and cats. J Vet Dent 2002;19:122-126.
PUBMED | CROSSREF
2. Théon AP, Rodriguez C, Madewell BR. Analysis of prognostic factors and patterns of failure in dogs with malignant oral tumors treated with megavoltage irradiation. J Am Vet Med Assoc 1997;210:778-784.
PUBMED
3. Brissot HN, Edery EG. Use of indirect lymphography to identify sentinel lymph node in dogs: a pilot study in 30 tumours. Vet Comp Oncol 2017;15:740-753.
PUBMED | CROSSREF
4. Langenbach A, McManus PM, Hendrick MJ, Shofer FS, Sorenmo KU. Sensitivity and specificity of methods of assessing the regional lymph nodes for evidence of metastasis in dogs and cats with solid tumors. J Am Vet Med Assoc 2001;218:1424-1428.
PUBMED | CROSSREF
5. Nyman HT, Lee MH, McEvoy FJ, Nielsen OL, Martinussen T, Kristensen AT. Comparison of B-mode and Doppler ultrasonographic findings with histologic features of benign and malignant superficial lymph nodes in dogs. Am J Vet Res 2006;67:978-984.
PUBMED | CROSSREF
6. Nyman HT, O'Brien RT. The sonographic evaluation of lymph nodes. Clin Tech Small Anim Pract 2007;22:128-137.
PUBMED | CROSSREF
7. Seiler GS, Griffith E. Comparisons between elastographic stiffness scores for benign versus malignant lymph nodes in dogs and cats. Vet Radiol Ultrasound 2018;59:79-88.
PUBMED | CROSSREF
8. Johnson PJ, Elders R, Pey P, Dennis R. Clinical and magnetic resonance imaging features of inflammatory versus neoplastic medial retropharyngeal lymph node mass lesions in dogs and cats. Vet Radiol Ultrasound 2016;57:24-32.
PUBMED | CROSSREF

9. Ballegeer EA, Adams WM, Dubielzig RR, Paoloni MC, Klauer JM, Keuler NS. Computed tomography characteristics of canine tracheobronchial lymph node metastasis. Vet Radiol Ultrasound 2010;51:397-403.
PUBMED | CROSSREF

10. Grimes JA, Secrest SA, Northrup NC, Saba CF, Schmiedt CW. Indirect computed tomography lymphangiography with aqueous contrast for evaluation of sentinel lymph nodes in dogs with tumors of the head. Vet Radiol Ultrasound 2017;58:559-564.
PUBMED | CROSSREF

11. Stahle JA, Larson MM, Rossmeisl JH, Dervisis N, Neelis D. Diffusion weighted magnetic resonance imaging is a feasible method for characterizing regional lymph nodes in canine patients with head and neck disease. Vet Radiol Ultrasound 2019;60:176-183.
PUBMED | CROSSREF

12. Bhatia KS, Cho CC, Yuen YH, Rasalkar DD, King AD, Ahuja AT. Real-time qualitative ultrasound elastography of cervical lymph nodes in routine clinical practice: interobserver agreement and correlation with malignancy. Ultrasound Med Biol 2010;36:1990-1997.
PUBMED | CROSSREF

13. Tan R, Xiao Y, He Q. Ultrasound elastography: its potential role in assessment of cervical lymphadenopathy. Acad Radiol 2010;17:849-855.
PUBMED | CROSSREF

14. Thomas A, Kümmel S, Fritzsche F, Warm M, Ebert B, Hamm B, Fischer T. Real-time sonoelastography performed in addition to B-mode ultrasound and mammography: improved differentiation of breast lesions? Acad Radiol 2006;13:1496-1504.
PUBMED | CROSSREF

15. Burnside ES, Hall TJ, Sommer AM, Hesley GK, Sisney GA, Svensson WE, Fine JP, Jiang J, Hangiandreou NJ. Differentiating benign from malignant solid breast masses with US strain imaging. Radiology 2007;245:401-410.
PUBMED | CROSSREF

16. Regner DM, Hesley GK, Hangiandreou NJ, Morton MJ, Nordland MR, Meixner DD, Hall TJ, Farrell MA, Mandrekar JN, Harmsen WS, Charboneau JW. Breast lesions: evaluation with US strain imaging--clinical experience of multiple observers. Radiology 2006;238:425-437.
PUBMED | CROSSREF

17. Desmots F, Fakhry N, Mancini J, Reyre A, Vidal V, Jacquier A, Santini L, Moulin G, Varoquaux A. Shear wave elastography in head and neck lymph node assessment: image quality and diagnostic impact compared with B-mode and Doppler ultrasonography. Ultrasound Med Biol 2016;42:387-398.
PUBMED | CROSSREF

18. Alam F, Naito K, Horiguchi J, Fukuda H, Tachikake T, Ito K. Accuracy of sonographic elastography in the differential diagnosis of enlarged cervical lymph nodes: comparison with conventional B-mode sonography. AJR Am J Roentgenol 2008;191:604-610.
PUBMED | CROSSREF

19. Belotta AF, Gomes MC, Rocha NS, Melchert A, Giuffrida R, Silva JP, Mamprim MJ. Sonography and sonoelastography in the detection of malignancy in superficial lymph nodes of dogs. J Vet Intern Med 2019;33:1403-1413.
PUBMED | CROSSREF

20. Moon WK, Choi JW, Cho N, Park SH, Chang JM, Jang M, Kim KG. Computer-aided analysis of ultrasound elasticity images for classification of benign and malignant breast masses. AJR Am J Roentgenol 2010;195:1460-1465.
PUBMED | CROSSREF

21. Nakajima T, Inage T, Sata Y, Morimoto J, Tagawa T, Suzuki H, Iwata T, Yoshida S, Nakatani Y, Yoshino I. Elastography for predicting and localizing nodal metastases during endobronchial ultrasound. Respiration 2015;90:499-506.
PUBMED | CROSSREF

22. Viera AJ, Garrett JM. Understanding interobserver agreement: the kappa statistic. Fam Med 2005;37:360-363.
PUBMED

23. Nyman HT, Kristensen AT, Skovgaard IM, McEvoy FJ. Characterization of normal and abnormal canine superficial lymph nodes using gray-scale B-mode, color flow mapping, power, and spectral Doppler ultrasonography: a multivariate study. Vet Radiol Ultrasound 2005;46:404-410.
PUBMED | CROSSREF

24. De Swarte M, Alexander K, Rannou B, D'Anjou MA, Blond L, Beauchamp G. Comparison of sonographic features of benign and neoplastic deep lymph nodes in dogs. Vet Radiol Ultrasound 2011;52:451-456.
PUBMED | CROSSREF

25. Carlsen JF, Ewertsen C, Sletting S, Talman ML, Vejborg I, Bachmann Nielsen M. Strain histograms are equal to strain ratios in predicting malignancy in breast tumours. PLoS One 2017;12:e0186230.
PUBMED | CROSSREF

26. Chiorean L, Barr RG, Braden B, Jenssen C, Cui XW, Hocke M, Schuler A, Dietrich CF; Current Clinical Applications and Literature Review. Transcutaneous ultrasound: elastographic lymph node evaluation. Ultrasound Med Biol 2016;42:16-30.
PUBMED | CROSSREF

27. Wojcinski S, Dupont J, Schmidt W, Cassel M, Hillemanns P. Real-time ultrasound elastography in 180 axillary lymph nodes: elasticity distribution in healthy lymph nodes and prediction of breast cancer metastases. BMC Med Imaging 2012;12:35.
PUBMED | CROSSREF

28. Dietrich CF, Cantisani V. Current status and perspectives of elastography. Eur J Radiol 2014;83:403-404.
PUBMED | CROSSREF